Journal of Zhejiang University SCIENCE
ISSN 1009-3095
http://www.zju.edu.cn/jzus
E-mail: jzus@zju.edu.cn

Design of capacitance sensor system for void fraction measurement

LIU Yi-ping (刘夷平)†, NIU Gang (牛 刚), WANG Jing (王 经)

(*School of Mechanical and Power Engineering, Shanghai Jiao Tong University, Shanghai 200030, China*)

†E-mail: Cloud3@sjtu.edu.cn

Received Sept. 7, 2005; revision accepted Sept. 20, 2005

Abstract: Simulation and optimization were applied to a capacitive sensor system based on electrical tomography technology. Sensors, consisting of Morgantown Energy Technology Center (METC) axial synchro driving guard electrodes and two sets of detecting electrodes, make it possible to obtain simultaneously two groups of signals of the void fraction in oil-gas two-phase flow. The computational and experimental results showed that available sensors, charactered by high resolution and fast real-time response can be used for real-time liquid-gas two-phase flow pattern determination.

Key words: Tomography, Capacitance sensors, Finite element
doi:10.1631/jzus.2005.A1424 **Document code:** A **CLC number:** TB126

INTRODUCTION

Oil-gas multiphase transport technology, including multiphase pressurization, multiphase flowmeter and multiphase flow control, has become very effective as an economic and reliable method for seabed oil exploitation. During the design of mixing transport system, prediction of pressure drop, heat transfer coefficients and void fraction is needed, so flow pattern identification is necessary. Among flow parameters, void fraction, defined as the cross section fraction occupied by gas, i.e. $\alpha=A_g/A$, is the most effective one reflecting flow pattern characteristics (Hewitt, 1982). Although much effort has been made on the theoretical computation and empirical formula derived from experiment, it is unsuitable for applying them to oil-gas two-phase flow system in many cases where actual measurement is required.

Quick Close Value (QCV) might be the commonest method to measure void fraction directly (Hewitt, 1978). Two synchro driving electromagnetic valves are mounted on both ends of the test pipe. As fully developed two-phase flow is achieved, the two valves are closed simultaneously, so that the average void fraction can be obtained by liquid/gas separation. However, failure to realize real-time measurement prevents its application in industrial production. X-ray absorption, based on X-ray attenuation principle, can provide accurate measurement, but the well known radioactive effect limits the use of this method to a few special fields. In recent years, there has been growing interest in flow imaging and research works based on neutron (Hussein and Meneley, 1986), gamma-ray (Kirouac *et al.*, 1999) and ultra sound (Plaskowski *et al.*, 1987) techniques have been reported. In this paper, since the phase component distribution varies in space and time in a statistically non-stationary manner, an electrical capacitive tomography (ECT) system has been employed to measure void fraction, it is one kind of process tomography technique, used comprehensively in medical imaging providing useful means for obtaining instantaneous information on distribution of components over a cross section. Beck *et al.*(1993) first proposed this technique which has been found to have considerable potential for use in process industry especially oil industry.

ECT system consists of three core parts (Fig.1):

* Project (No. 2002AA616050) supported by the Hi-Tech Research and Development Program (863) of China

capacitance sensors, data collection and control system and imaging reconstruction computer. The sensors transform two-phase flow distribution into capacitive values whose amplitude depends on the dielectric distribution over the cross section of pipeline. The data collection and control system receives them in all possible electrode pairs. Through A/D transformation, the values, as digital signal, are fed into the computer and a cross sectional image of the components distribution is reconstructed by using a linear backprojection (LBP) algorithm.

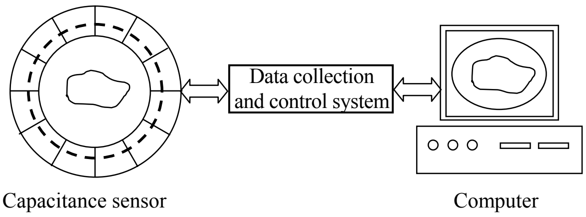

Fig.1 The basic flow imaging system

In this work, a capacitance sensor system for void fraction measurement in oil-gas two-phase flow pipeline is developed. According to the arrangement of the multielectrode circumferentially around the pipe there are four basic structures to be selected: (1) external electrodes with radial screens, (2) internal electrodes without radial screens, (3) external electrodes without radial screens, (4) internal electrodes with radial screens. Yang (1997) summarized their features. In terms of the axial guard electrodes, two major structures are available, one is multielectrode capacitive system with axial synchro driving guard electrodes developed by U.S. Department of Energy, Morgantown Energy Technology Center (METC), the other is multielectrode capacitive system with axial earthed guard electrodes developed by the University of Manchester Institute of Science and Technology (UMIST). METC system uses 16 evenly spaced, circumferentially located electrodes at each of four levels evenly spaced along the axis of a 6-inch diameter fluidized bed as the density-sensing elements. During the measurement, the erasable programmable read-only memory (EPROM) section of the scan control system is programmed to produce electrode voltage excitation patterns that allow the electrically guarded measurement of the current between all possible pairs of oppositely excited electrodes simultaneously at each level. UMIST system consists of a source electrode (connected to the driving voltage source), a detecting electrode (connected to the virtual earth input of the capacitance measuring circuit) and an earthed screen to shield the electrode plates from interference by external electrical fields. In addition, multielectrode capacitive system without axial guard electrodes (non-guard) is studied as a candidate. Moreover, the system design parameters, including the pipe wall permittivity (ε_{pw}), the permittivity of the conveyed phase (ε), the length of axial guard electrode plate, the pipe wall thickness (R_2-R_1) and the electrode angular size (θ), have effects on the sensitivities distribution's influence on the measurement. Therefore, the analysis of these parameters is involved in the present simulation.

The reconstructed image quality and the multielectrode capacitive system's performance depend on the uniformity of sensibility distribution between electrode pairs (Khan and Abdullah, 1993). To determine the spatial sensitivity distribution over the pipe cross section and to study the static responses of the system due to different flow regimes, a numerical simulation must be used to optimize the design parameters and the system performance of the capacitive systems described above. FE modelling was chosen in this research because its mesh can be designed to fit complex geometries and the system capacitance is easy to compute from the known electrical potential distributions on the system boundary.

FINITE ELEMENT MODELLING OF CAPACITANCE SENSOR SYSTEM

In the past, two-dimensional FE modelling of capacitance sensor system was always adopted under the assumption that the fringing field effects due to the finite length of electrodes are negligible. This assumption implies that the electrode plates and screen are so long that the electric field distribution remains the same for any plane perpendicular to the axial direction of the pipe. However, it is not entirely suitable for most capacitance sensor systems, such as METC and UMIST. In order to get accurate prediction, a three-dimensional FE modelling was proposed. The basic model and FE mesh layout are shown in Fig.2. The fringing field effects are taken into account, and the other common assumptions are listed below:

(1) Flow component distribution of a two-phase

flow does not change spatially along the pipe axial direction at least not within the electrode length.

(2) Permittivities of flow components remain constant.

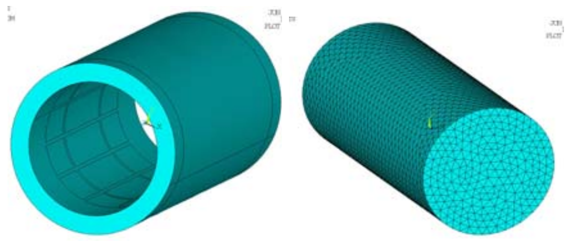

Fig.2 Finite element model of 12-electrode capacitive system with mesh layout

Under these two assumptions, the potential distribution over cross section can be calculated by Poisson equation with the given dielectric constant distribution. The Dirichlet boundary conditions are given below:

$$\begin{cases} \nabla\cdot[\varepsilon(x,y,z)\nabla\varphi(x,y,z)]=0 \\ \varphi(x,y,z)|_{(x,y,z)\in\Gamma_i}=U & (i=1,2,\cdots,11) \\ \varphi(x,y,z)|_{(x,y,z)\in\Gamma_j}=0 & (j=2,3,\cdots,12) \\ \varphi(x,y,z)|_{(x,y,z)\in\Gamma_s}=0 \end{cases} \tag{1}$$

where, Γ_s represent the computational domains belonging to the screen, and Γ_i and Γ_j are the spatial locations of ith electrode and jth electrode respectively, U is the potential difference between given electrodes. According to Thomson's theorem, for specified charges on each of the boundary segments, the stored electrostatic energy is minimum when each of the boundaries is a conductor, i.e., electrically charged particles arrange themselves so as to have the least energy. As a result, the numerical functional form of Eq.(1) is given as

$$\begin{cases} J_\varphi=\frac{1}{2}\iiint\limits_D \varepsilon(x,y,z)E^2\mathrm{d}V=\iiint\limits_D \frac{\varepsilon(x,y,z)}{2}\left[\left(\frac{\partial\varphi(x,y,z)}{\partial x}\right)^2 \right. \\ \left. +\left(\frac{\partial\varphi(x,y,z)}{\partial y}\right)^2+\left(\frac{\partial\varphi(x,y,z)}{\partial z}\right)^2\right]\mathrm{d}x\mathrm{d}y\mathrm{d}z=\min \\ \varphi(x,y,z)|_{(x,y,z)\in\Gamma_i}=U & (i=1,\ 2,\ \cdots,\ 11) \\ \varphi(x,y,z)|_{(x,y,z)\in\Gamma_j}=0 & (j=2,\ 3,\ \cdots,\ 12) \\ \varphi(x,y,z)|_{(x,y,z)\in\Gamma_s}=0 \end{cases} \tag{2}$$

where D is the space inside shield screen. As mentioned above, one task in current work is to facilitate the selection of capacitance sensor system and optimizing system design parameter. Therefore, it goes along a forward solving process. After the potential distribution is obtained, Gauss law with numerical integral form, i.e. Eq.(3), is applied to calculate the sense charge on the jth electrode.

$$\begin{aligned} q_{ij} &= \iiint\limits_{V_j} \varepsilon(x,y,z)\boldsymbol{E}(x,y,z)\ \mathrm{d}\boldsymbol{V} \\ &= -\iiint\limits_{V_j} \varepsilon(x,y,z)\nabla\varphi(x,y,z)\ \mathrm{d}\boldsymbol{V} \end{aligned} \tag{3}$$

where V_j is the volume enveloping the electrode j. Then the capacitance of electrode pairs i-j can be calculated from Eq.(4):

$$C_{ij}=q_{ij}/U \quad (i=1,\ 2,\ \cdots,\ 11;\ j=2,\ 3,\ \cdots,\ 12) \tag{4}$$

RESULTS AND DISCUSSION

Spatial distribution of three capacitive systems

Fig.3 shows the potential distribution in the center axial section in three sensors. The part between two solid lines represents the detecting electrode domain. In this figure, potential distribution discrepancy is shown by equipotential contours, uniformity in potential distribution appears in METC system, while UMIST contours and non-guard system seem to be uneven. This computational result means that electrical fields in UMIST and non-screen system tend to disperse along the axial direction and that the lines of the electric field are perpendicular to the equipotential contours. In contrast, the depressiveness in the METC system seems imperceptible. Therefore, as the permittivities of flow components keep constant, it can be concluded that the value attributed to a measurand by METC system should be closer to the simulation result than that by UMIST and non-guard system, and such conclusion leads to the selection of the METC system.

Effect of METC system guard electrode length on the spatial potential distribution

The potential distribution in the center axial section of five different lengths of guard electrode plate, i.e. 20 mm, 30 mm, 50 mm, 70 mm and 100 mm, are shown in Fig.4. The two solid lines have the same meaning as mentioned above. Although the potential distribution between the excited electrode and detecting electrode tends to be even with increasing length of guard electrode plate, no evident change of the potential distribution between the two detecting electrode plates was noticed after the plate length exceeded a certain value. On the other hand, if the plate becomes too long, the cost of the overall capacitive system will increase. So, for the pipeline with 125 mm interior diameter, 50 mm long guard electrode is enough for shield.

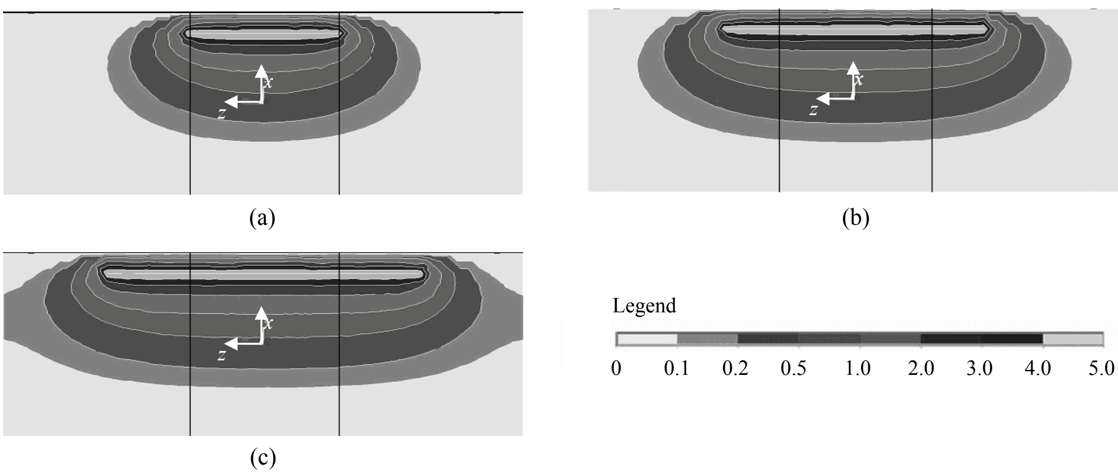

Fig.3 Potential distribution in the center axial section for three types of sensors, *L* is the length of electrode plate
(a) Non-guard electrode; (b) UMIST (L=50 mm); (c) METC (L=50 mm)

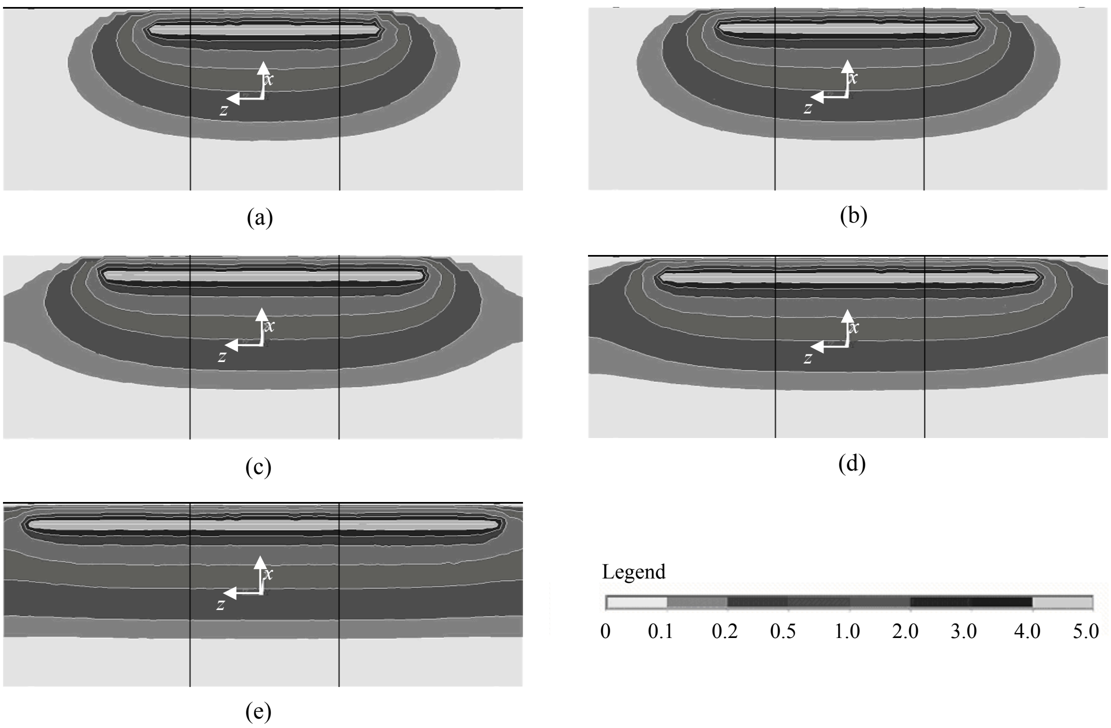

Fig.4 Potential distribution in the center axial section for five different lengths of guard electrode plate
(a) L=20 mm; (b) L=30 mm; (c) L=50 mm; (d) L=70 mm; (e) L=100 mm

Effects of the sensors layout

In this section, the comparisons between the internal and the external capacitance sensor systems are given on two aspects, full pipe and empty pipe. First, the potential distribution over cross section with internal electrodes is shown in Fig.5. It seems that no distinct variation has been found between full pipe and empty pipe. However, according to the conclusion given by Hussein and Meneley (1986), the pipe wall thickness plays an import part in capacitance sensitivity homogeneity and the consideration about thickness effect is indispensable. Comparison of capacitance values of external and internal sensors is presented in Table 1. Some system design parameters are given below:

Pipe wall permittivity: ε_{pw}=3.45; Electrode angle: θ=27°; L=100 mm; Internal: R_1=62.5 mm, R_2=79.5 mm, R_3=0 mm; External: R_1=62.5 mm, R_2=79.5 mm, R_3=99.5 mm.

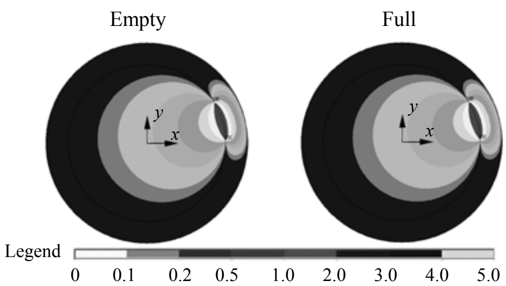

Fig.5 Potential distribution in the radial section of sensors with internal electrode

Table 1 shows that when the electrode geometry is fixed, external system corresponds to larger stationary capacitance values in empty pipe, while in full pipe, the two types of sensors had almost the same capacitance values. Descending tendency of capacitance variation between full and empty pipe was found in the internal system. Note that the capacitance variation between adjoining electrodes, such as electrodes 1 and 2 has a negative value, this behavior results from the so-called soft field effect, in other words, after an ECT system applies an excitation voltage or current, the sensing field is distorted by the target object(s), so that a non-uniform field is induced. The relationship among the capacitance of an electrode pair, C_i, the measured sensitivity distribution function, $S_i(x, y, \varepsilon(x, y))$, and the dielectric distribution in the pipe, $\varepsilon(x, y)$, is expressed as:

$$C_i = \iint_D \varepsilon(x, y) S_i(x, y,\ \varepsilon(x, y))\ \mathrm{d}x\mathrm{d}y \quad (5)$$

where D is the cross section of the pipe. It should be noted that C_i depends on the dielectric distributions in the area where the sensitivity is positive, while negative sensing area corresponding to soft field should be eliminated during the image reconstruction process, this means that the number of image data available decreases and the image quality is unsatisfactory for predicting the final distribution of the two components. Therefore, internal capacitive sensor system is more suitable than the external one for the current design.

Basic design scheme

A capacitance sensor system employed in the multiphase flow experimental loop at Daqing oil log detection center was proposed for optimization using FE modelling. One m long, 130 mm interior diameter, 14 mm wall thickness acrylic pipe was used in the main frame. Twelve-electrode internal sensors with axial synchro driving guard electrodes (METC) consisting of two sets of detecting electrodes were adopted. The basic structure's schematic diagram is shown in Fig.6. The 10 cm long, 3.2 cm wide, 0.1 mm thick detecting electrodes fabricated from brass are mounted flush with the interior wall with a set of 12 electrodes symmetrically spaced around the circumference of the pipe making up one imaging level. Two sets, between which one set of 10 mm long guard electrode is located, are 10 cm apart. The two 5 cm

Table 1 Comparison of capacitance values of internal and external sensors

		C_{1-2}	C_{1-3}	C_{1-4}	C_{1-5}	C_{1-6}	C_{1-7}
Internal	Empty	2.409454	0.090151	0.041005	0.026662	0.021228	0.019751
	Full	3.604968	0.224051	0.102713	0.066788	0.053177	0.049480
	ΔC	1.195514	0.133900	0.061708	0.040126	0.0131949	0.029729
External	Empty	3.555181	0.163814	0.050208	0.029279	0.0225609	0.020838
	Full	3.541350	0.267691	0.111908	0.070372	0.055302	0.051303
	ΔC	0.013831	0.103877	0.061700	0.041093	0.032742	0.030465

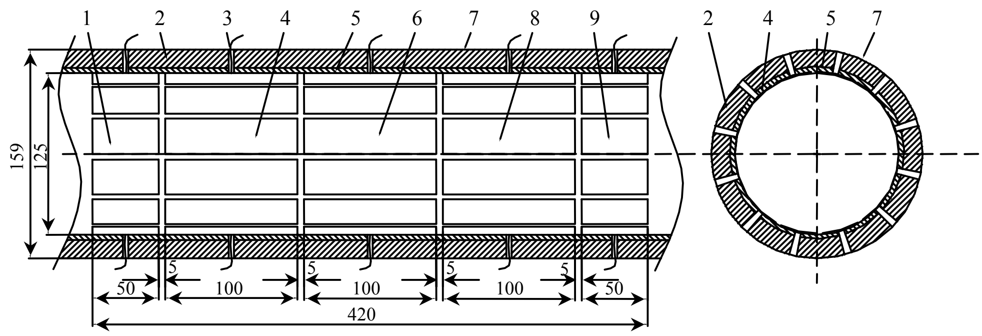

Fig.6 Schematic diagram of the capacitance sensor system
1, 6, 9: Axial guard electrodes; 2: Acrylic pipe; 3: Lead wire; 4, 8: Detecting electrode; 5: Scaleboard; 7: Screen

wide by 10 cm long guard electrode sets are located flush against the interior wall of the pipe, spaced 5 mm left and right of the horizontal edges of two sensing electrode sets. These electrodes serve to shape and minimize interaction by the electrode field linking pairs of detecting electrodes during measurement.

Layout of electrode sets

Another purpose of the designed system is to give an accurate layout for electrodes since the asymmetric layout tends to lead to adverse performance of the overall system. As internal capacitance sensors (two sets of detecting electrodes and three sets of guard electrodes, totally 60 electrodes) are involved in the current system, special treatment is needed. All the electrodes are fixed on a polyethylene scaleboard beforehand, and then the scaleboard is rolled up and attached to the interior wall of the pipe.

Rest of the design

Since the electrodes are placed inside the pipe, Sixty 10 mm diameter holes were drilled on the acrylic pipe surface, from which wire leads welded to the electrodes came out. The acrylic pipe was coated with 0.1 mm thick aluminum plate as shield screen to prevent electromagnetic interference from outside (Fig.7), so adequate grounding was necessary.

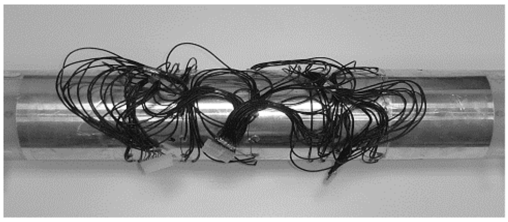

Fig.7 Photo of capacitance sensor system

CONCLUSION

Three types of capacitance sensors were simulated and optimized by FE modelling techniques described in this paper. As consequence, a prototype of 12-electrode internal sensors with axial synchro driving guard electrodes (METC) was selected as the first part of the ECT system used in oil-gas two-phase flow void fraction measurement. It was shown that performance evaluation and characterization of the capacitance sensor system could be achieved effectively by using FE modeling, and simulation results, such as dielectric distribution, might serve as reference material for future systems.

References

Beck, M.S., 1993. PC-Opera User Guide and Reference Manual. Vector Field Limited, Oxford, UK.

Hewitt, G.F., 1978. Measurement of Two-phase Flow Parameters. Academic Press, London.

Hewitt, G.F., 1982. Handbook of Multiphase System. Hemisphere Publishing, Washington.

Hussein, E.M.A., Meneley, D.A., 1986. Single-exposure neutron tomography of two-phase flow. *Int. J. Multiphase Flow*, **12**:1-34.

Khan, S.H., Abdullah, F., 1993. Finite element modelling of multielectrode capacitive systems for flow imaging. *IEE Proceedings G*, **140**(3):216-222.

Kirouac, G.J., Trabold, T.A., Vassallo, P.F., Moore, W.E., Kumar, R., 1999. Instrumentation development in two-phase flow. *Experimental Thermal and Fluid Science*, **20**(2):79-93.

Plaskowski, A.B., Beck, M.S., Krawaczynski, J.S., 1987. Flow imaging for multi-component measurement. *Tran. Inst. Meas. Control*, **9**:108-112.

Yang, W.Q., 1997. Modelling of capacitance tomography sensors. *IEE Proceedings-Sci. Meas.*, **144**(5):203-208.